Observation of a New Ξ_b^- Resonance

R. Aaij *et al.*[*]
(LHCb Collaboration)

(Received 24 May 2018; published 15 August 2018)

From samples of pp collision data collected by the LHCb experiment at $\sqrt{s} = 7$, 8 and 13 TeV, corresponding to integrated luminosities of 1.0, 2.0 and 1.5 fb^{-1}, respectively, a peak in both the $\Lambda_b^0 K^-$ and $\Xi_b^0\pi^-$ invariant mass spectra is observed. In the quark model, radially and orbitally excited Ξ_b^- resonances with quark content bds are expected. Referring to this peak as $\Xi_b(6227)^-$, the mass and natural width are measured to be $m_{\Xi_b(6227)^-} = 6226.9 \pm 2.0 \pm 0.3 \pm 0.2$ MeV/c^2 and $\Gamma_{\Xi_b(6227)^-} = 18.1 \pm 5.4 \pm 1.8$ MeV/c^2, where the first uncertainty is statistical, the second is systematic, and the third, on $m_{\Xi_b(6227)^-}$, is due to the knowledge of the Λ_b^0 baryon mass. Relative production rates of the $\Xi_b(6227)^- \to \Lambda_b^0 K^-$ and $\Xi_b(6227)^- \to \Xi_b^0\pi^-$ decays are also reported.

DOI: 10.1103/PhysRevLett.121.072002

In the constituent quark model [1,2], baryonic states form multiplets according to the symmetry of their flavor, spin, and spatial wave functions. The masses, widths, and decay modes of these states give insight into their internal structure [3]. The Ξ_b^0 and Ξ_b^- states form an isodoublet of bsq bound states, where q is a u or d quark, respectively. Three such isodoublets, which are neither radially nor orbitally excited, should exist [4], and include one with spin $j_{qs} = 0$ and $J^P = (1/2)^+$ (Ξ_b), a second with $j_{qs} = 1$ and $J^P = (1/2)^+$ (Ξ_b'), and a third with $j_{qs} = 1$ and $J^P = (3/2)^+$ (Ξ_b^*). Here, j_{qs} is the spin of the light diquark system qs, and J^P represents the spin and parity of the state. Three of the four $j_{qs} = 1$ states have been recently observed through their decays to $\Xi_b^0\pi^-$ and $\Xi_b^-\pi^+$ [5–7].

Beyond these lowest-lying states, a spectrum of heavier states is expected [8–23], where there are either radial or orbital excitations amongst the constituent quarks. The only such states discovered thus far in the b-baryon sector are the $\Lambda_b(5912)^0$ and $\Lambda_b(5920)^0$ resonances [24], which are consistent with being orbital excitations of the Λ_b^0 baryon.

In this Letter, we report the first observation of a new state, decaying into both $\Lambda_b^0 K^-$ and $\Xi_b^0\pi^-$, using samples of pp collision data collected with the LHCb experiment at 7, 8, and 13 TeV, corresponding to integrated luminosities of 1.0, 2.0, and 1.5 fb^{-1}, respectively. The observation of these decays is consistent with the strong decay of a radially or orbitally excited Ξ_b^- baryon, hereafter referred to as $\Xi_b(6227)^-$. Charge-conjugate processes are implicitly included throughout this Letter.

The mass and width of the $\Xi_b(6227)^-$ baryon are measured using the $\Lambda_b^0 K^-$ mode, where the Λ_b^0 baryon is detected through its fully reconstructed hadronic (HAD) decay to $\Lambda_c^+\pi^-$. Larger samples of semileptonic (SL) Λ_b^0 and Ξ_b^0 decays are used to measure the production ratios

$$R(\Lambda_b^0 K^-) \equiv \frac{f_{\Xi_b(6227)^-}}{f_{\Lambda_b^0}} \mathcal{B}(\Xi_b(6227)^- \to \Lambda_b^0 K^-), \quad (1)$$

$$R(\Xi_b^0\pi^-) \equiv \frac{f_{\Xi_b(6227)^-}}{f_{\Xi_b^0}} \mathcal{B}(\Xi_b(6227)^- \to \Xi_b^0\pi^-), \quad (2)$$

where $f_{\Xi_b(6227)^-}$, $f_{\Xi_b^0}$, and $f_{\Lambda_b^0}$ are the fragmentation fractions of a b quark into each baryon and $\mathcal{B}$ represents a branching fraction. Here, the Λ_b^0 and Ξ_b^0 baryons are detected using $\Lambda_b^0 \to \Lambda_c^+\mu^- X$ and $\Xi_b^0 \to \Xi_c^+\mu^- X$ decays, where X represents undetected particles. Throughout the text, H_b^0 (H_c^+) is used to designate either a Λ_b^0 or Ξ_b^0 (Λ_c^+ or Ξ_c^+) baryon. Owing to much larger branching fractions, the SL signal yields are about an order of magnitude larger than that of any fully hadronic final state, which enables the observation of the $\Xi_b(6227)^- \to \Xi_b^0\pi^-$ mode. The SL decays are not used in the $\Xi_b(6227)^-$ mass or width determination, as they have larger systematic uncertainties due to modeling of the mass resolution.

The LHCb detector [25,26] is a single-arm forward spectrometer covering the pseudorapidity range $2 < \eta < 5$, designed for the study of particles containing b or c quarks [25,26]. Events are selected online by a trigger, which consists of a hardware stage, based on information from the calorimeter and muon systems, followed by a software stage, which applies a full event reconstruction [27,28].

[*]Full author list given at the end of the Letter.

Simulated data samples are produced using the software packages described in Refs. [29–35].

Samples of Λ_b^0 (Ξ_b^0) are formed from $\Lambda_c^+\pi^-$ and $\Lambda_c^+\mu^-$ ($\Xi_c^+\mu^-$) combinations, where Λ_c^+ and Ξ_c^+ decays are reconstructed in the $pK^-\pi^+$ final state. The H_c^+ decay products must have particle identification (PID) information consistent with the given particle hypothesis, and be inconsistent with originating from a primary vertex (PV) by requiring each to have large $\chi^2_{\rm IP}$ with respect to all PVs in the event. Here $\chi^2_{\rm IP}$ is the difference in χ^2 of the vertex fit of a given PV when the particle (here p, K^- or π^+) is included or excluded from the fit. The H_c^+ candidate must have a fitted vertex significantly displaced from all PVs in the event and have an invariant mass within 60 MeV/c^2 of the known H_c^+ mass.

The H_c^+ background is dominated by random combinations of tracks from nonsignal b-hadron decays. In the Ξ_c^+ sample, about 15% of this background is due to misidentified $D^+ \to K^-\pi^+\pi^+$, $D^+ \to K^+K^-\pi^+$, $D_s^+ \to K^+K^-\pi^+$, and $D^{*+} \to (D^0 \to K^-\pi^+)\pi^+$ decays. These cross-feed contributions are suppressed by employing tighter PID requirements on candidates that are consistent with being one of these charm mesons, with only a 1% loss of signal efficiency. These tighter requirements are not applied to the Λ_c^+ sample, as the cross-feed contributions are negligible.

Muon (pion) candidates with transverse momentum $p_{\rm T} > 1$ GeV/c (0.5 GeV/c) and large $\chi^2_{\rm IP}$ are combined with H_c^+ candidates to form the H_b^0 samples. Each H_b^0 decay vertex is required to be significantly displaced from all PVs in the event. For the $\Lambda_b^0 \to \Lambda_c^+\pi^-$ decay, the reconstructed Λ_b^0 trajectory must point back to one of the PVs in the event; only a very loose pointing requirement is imposed on the SL decay due to the momentum carried by the undetected particles. To reduce background in the SL decay samples, the z coordinates of the H_c^+ and H_b^0 decay vertices are required to satisfy $z(H_c^+) - z(H_b^0) > -0.05$ mm, where z is measured along the beam direction. Candidates that satisfy the invariant mass requirements, $5.2 < M(\Lambda_c^+\pi^-) < 6.0\,{\rm GeV}/c^2$ or $M(H_c^+\mu^-) < 8\,{\rm GeV}/c^2$, are retained, where M designates the invariant mass of the system of indicated particle(s).

To further suppress background in the $\Xi_b^0 \to \Xi_c^+\mu^-X$ sample, a boosted decision tree (BDT) discriminant [36,37] is used. The BDT exploits 14 input variables: the χ^2 values of the fitted Ξ_c^+ and Ξ_b^0 decay vertices, and the momentum, $p_{\rm T}$, $\chi^2_{\rm IP}$, and a PID variable for each Ξ_c^+ final-state particle. Simulated signal decays and background from the Ξ_c^+ mass sidebands, $30 < |M(pK^-\pi^+) - m_{\Xi_c^+}| < 60$ MeV/c^2, in data are used to train the BDT, where m refers to the known mass of the indicated particle [38]. The PID response for final-state hadrons in the signal decay is obtained from large $\Lambda \to p\pi^-$ and $D^{*+} \to (D^0 \to K^-\pi^+)\pi^+$ calibration samples in data, which is weighted to reproduce the kinematics of the signal. The chosen requirement on the BDT response provides an efficiency of about 90% (40%) on the signal (background).

Figure 1 shows the mass spectra for $\Lambda_b^0 \to \Lambda_c^+\pi^-$, $\Lambda_c^+ \to pK^-\pi^+$ (from $\Lambda_b^0 \to \Lambda_c^+\mu^-X$) and $\Xi_c^+ \to pK^-\pi^+$ (from $\Xi_b^0 \to \Xi_c^+\mu^-X$) candidates. For the $\Lambda_b^0 \to \Lambda_c^+\pi^-$ mode, a peak at the known Λ_b^0 mass is seen. For the SL modes, the Λ_c^+ and Ξ_c^+ mass peaks are used to determine the number of Λ_b^0 and Ξ_b^0 baryon decays, as the combinatorial background from random $H_c^+\mu^-$ combinations is at the 1% level. The mass spectra are fit with the sum of two Gaussian functions with a common mean to represent the signal component and an exponential background function. The yields are given in Table I.

To form $\Xi_b(6227)^-$ candidates, a Λ_b^0 (Ξ_b^0) candidate is combined with a K^- (π^-) meson that has small $\chi^2_{\rm IP}$, consistent with being produced in the strong decay of the $\Xi_b(6227)^-$ resonance. Only H_b^0 candidates satisfying $|M(\Lambda_c^+\pi^-)_{\rm HAD} - m_{\Lambda_b^0}| < 60$ MeV/c^2, $|M(pK^-\pi^+)_{\rm SL} - m_{\Lambda_c^+}| < 15$ MeV/c^2, and $|M(pK^-\pi^+)_{\rm SL} - m_{\Xi_c^+}| < 18$ MeV/c^2 are considered, where HAD and SL indicate the sample from which the mass is determined. We require $p_{\rm T}^{K^-} > 800$ MeV/c and $p_{\rm T}^{\pi^-} > 900$ MeV/c, based on an optimization of the expected statistical uncertainty on the $\Xi_b(6227)^-$ signal yield, using simulation to model the signal and either wrong-sign ($\Lambda_b^0K^+$, $\Xi_b^0\pi^+$) or $\Xi_b(6227)^-$ mass sideband samples in data to model the background. After all selections the dominant source of background is due to combinations of real Λ_b^0 (Ξ_b^0) decays with a random K^- (π^-) meson. All candidates satisfying these selections are retained.

To improve the resolution on the $\Xi_b(6227)^-$ mass, we use the mass differences $\delta m_K \equiv M(\Lambda_b^0K^-) - M(\Lambda_b^0)$ and $\delta m_\pi \equiv M(\Xi_b^0\pi^-) - M(\Xi_b^0)$, for the $\Lambda_b^0K^-$ and $\Xi_b^0\pi^-$ final states, respectively. The $\delta m_{K(\pi)}$ resolution is obtained from simulated $\Xi_b(6227)^-$ decays, where the decay width is set to a negligible value. For the $\Lambda_b^0 \to \Lambda_c^+\pi^-$ mode, the δm_K resolution model is approximately Gaussian with a width of 2.4 MeV/c^2. For the SL decays, the missing momentum, $p_{\rm miss}$, is estimated by assuming it is carried by a zero-mass particle that balances the momentum transverse to the H_b^0 direction (formed from its decay vertex and PV), and satisfies the mass constraint $(p_{H_c^+} + p_{\mu^-} + p_{\rm miss})^2 = m^2_{H_b^0}$. Mass resolution shape parameters are obtained by fitting the $\delta m_{K(\pi)}$ spectra from simulated decays, which include contributions from excited charm baryons and final states with τ^- leptons. The core of the resolution function has a half-width at half-maximum of about 20 MeV/c^2, and has a tail toward larger mass (see Supplemental Material [39]). The obtained shape parameters are fixed in the fits to data.

The δm_K and δm_π spectra in data are shown in Fig. 2. The $\Xi_b(6227)^-$ mass and width are obtained from a simultaneous unbinned maximum-likelihood fit to the

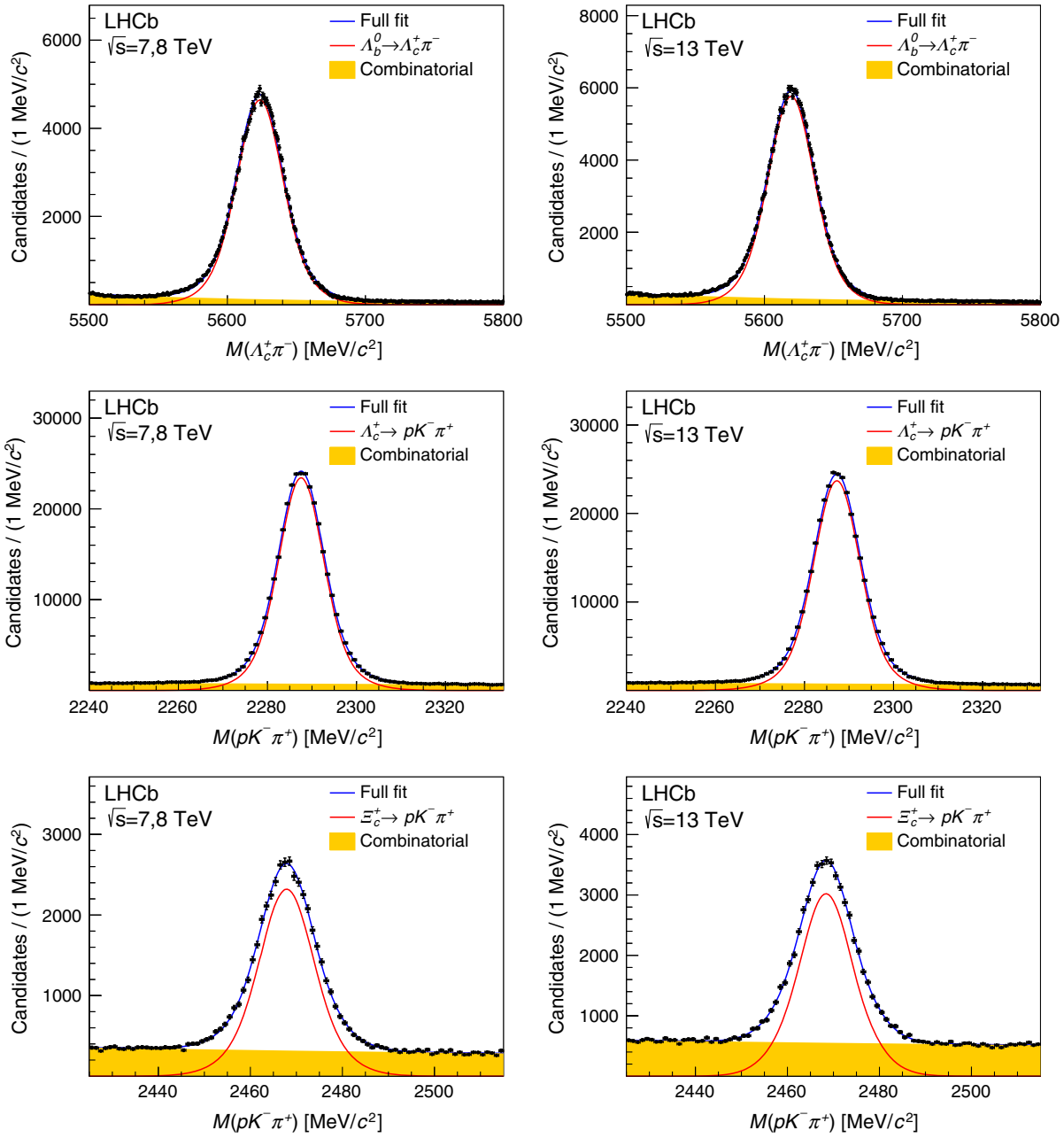

FIG. 1. Invariant mass spectra for (top) $\Lambda_b^0 \to \Lambda_c^+ \pi^-$, (middle) Λ_c^+ from $\Lambda_b^0 \to \Lambda_c^+ \mu^- X$, and (bottom) Ξ_c^+ from $\Xi_b^0 \to \Xi_c^+ \mu^- X$ candidate decays. The left column is for 7, 8 TeV and the right is for 13 TeV data. Fits are overlaid, as described in the text. Here, the $\Lambda_b^0 \to \Lambda_c^+ \mu^- X$ mode has been prescaled by a factor of 10.

TABLE I. Uncorrected $\Xi_b(6227)^-$ and H_b^0 signal yields for 7, 8, and 13 TeV data. The H_b^0 yields are limited to the signal regions used to form $\Xi_b(6227)^-$ candidates (see text).

$\Xi_b(6227)^-$	7,8 TeV		13 TeV	
Final state	$N(\Xi_b(6227)^-)$	$N(H_b^0)$ [10^3]	$N(\Xi_b(6227)^-)$	$N(H_b^0)$ [10^3]
$(\Lambda_b^0)_{\rm HAD} K^-$	170 ± 53	204.6 ± 0.5	215 ± 63	252.7 ± 0.6
$(\Lambda_b^0)_{\rm SL} K^-$	2772 ± 325	3133 ± 6	3701 ± 432	3226 ± 6
$(\Xi_b^0)_{\rm SL} \pi^-$	351 ± 68	36.6 ± 0.3	274 ± 73	46.5 ± 0.3

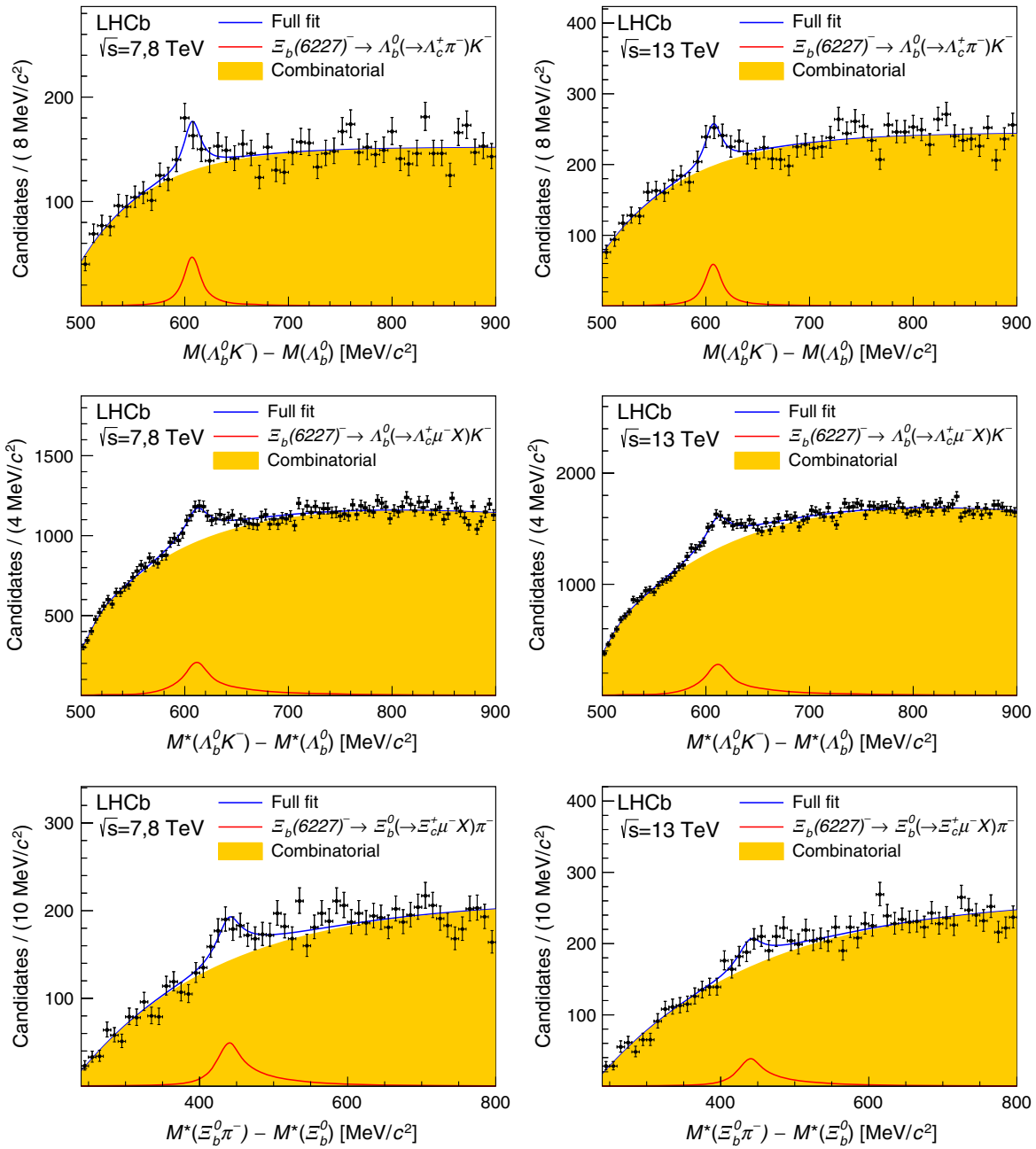

FIG. 2. Spectra of mass differences for $\Xi_b(6227)^-$ candidates, reconstructed in the final states (top) $\Lambda_b^0 K^-$, with $\Lambda_b^0 \to \Lambda_c^+ \pi^-$, (middle) $\Lambda_b^0 K^-$, with $\Lambda_b^0 \to \Lambda_c^+ \mu^- X$, and (bottom) $\Xi_b^0 \pi^-$, with $\Xi_b^0 \to \Xi_c^+ \mu^- X$, along with the results of the fits. The left column is for 7, 8 TeV and the right is for 13 TeV data. The symbol M^* represents the mass after the constraint $(p_{H_c^+} + p_{\mu^-} + p_{\rm miss})^2 = m^2_{H_b^0}$ is applied, as described in the text.

δm_K spectra in 7, 8, and 13 TeV data, using the $\Lambda_b^0 \to \Lambda_c^+ \pi^-$ mode. The signal shape is described by a P-wave relativistic Breit-Wigner function [40] with a Blatt-Weisskopf barrier factor [41], convoluted with a Gaussian resolution function of width 2.4 MeV/c^2. The mass and width are common parameters in the fit. The background shape is described by a smooth threshold function [42] with shape parameters that are freely and independently varied in the fits to the two data sets. A peak is observed in both data sets, with a mean $\delta m_K^{\rm peak} = 607.3 \pm 2.0$ MeV/c^2 and width $\Gamma_{\Xi_b(6227)^-} = 18.1 \pm 5.4$ MeV/c^2. The peak has a local statistical significance of about 7.9σ for the combined fit, based on the difference in log-likelihood values between a fit with zero signal and the best fit. The signal yields are given in Table I.

The $\Xi_b(6227)^- \to \Lambda_b^0 K^-$ decay with $\Lambda_b^0 \to \Lambda_c^+ \mu^- X$ is fit in a similar way, except for the different resolution function (see Supplemental Material [39]). A Gaussian constraint on

the width of $\Gamma_{\Xi_b(6227)^-} = 18.1 \pm 5.4$ MeV/c^2 is applied, as obtained from the fit to the hadronic mode, and the mean is freely varied. A peak is observed at a mass difference of $610.8 \pm 1.0(\text{stat})$ MeV/c^2, which is consistent with that of the hadronic mode, and it contains a yield about 15 times larger, as expected. The statistical significance of this peak is about 25σ, thus clearly establishing this peaking structure.

The $\Xi_b^0\pi^-$ final state is investigated by examining the δm_π spectra in $\Xi_b(6227)^- \to \Xi_b^0\pi^-$ candidate decays, as shown in the bottom row of Fig. 2. The fit is performed in an analogous way to the δm_K spectra, except for a different resolution function (see Supplemental Material [39] for δm_π resolution). The fitted mean of 440 ± 5 MeV/c^2 is consistent with the value expected from the hadronic mode of $\delta m_K^{\text{peak}} + m_{\Lambda_b^0} - m_{\Xi_b^0} = 435 \pm 2$ MeV/c^2. The statistical significance of the peak is 9.2σ.

The production ratios are computed using

$$R(\Lambda_b^0 K^-) = \frac{N(\Xi_b(6227)^- \to \Lambda_b^0 K^-)}{\epsilon_{\text{rel}} N(\Lambda_b^0)} \kappa, \tag{3}$$

$$R(\Xi_b^0\pi^-) = \frac{N(\Xi_b(6227)^- \to \Xi_b^0\pi^-)}{\epsilon'_{\text{rel}} N(\Xi_b^0)} \kappa', \tag{4}$$

where N represents the yields in Table I, and $\epsilon_{\text{rel}}^{(\prime)}$ is the relative efficiency between the $\Xi_b(6227)^-$ and H_b^0 selections, reported in Table II. The quantity $\kappa^{(\prime)}$ represents corrections to the $N(H_b^0)$ SL signal yields to account for (i) random $H_c^+\mu^-$ combinations, (ii) cross-feed from $\Xi_b^- \to \Xi_c^+\mu^- X$ decays into the $\Xi_b^0 \to \Xi_c^+\mu^-$ sample, and (iii) slightly different integrated luminosities used for the $\Xi_b(6227)^-$ and H_b^0 samples. The contribution from random $H_c^+\mu^-$ combinations is estimated from a study of the wrong-sign ($H_c^+\mu^+$) and right-sign ($H_c^+\mu^-$) yields, from which a correction of 1.010 ± 0.002 to both $R(\Xi_b^0\pi^-)$ and $R(\Lambda_b^0 K^-)$ is found. Cross-feeds from SL Ξ_b^- decays, which must be subtracted from $N(\Xi_b^0)$, are inferred by adding a π^- meson to the $\Xi_c^+\mu^-$ candidate and searching for excited Ξ_c^0 states. Mass peaks associated with the $\Xi_c(2645)^0$ and $\Xi_c(2790)^0$ resonances are observed, although for the former about half is due to $\Xi_c(2815)^+ \to \Xi_c(2645)^0\pi^+$ decays, as determined through a study of the $\Xi_c^+\pi^+$ mass spectrum. Since the $\Xi_c(2815)^+\mu^-$ final state is predominantly from Ξ_b^0 decays, this contribution is not subtracted. After correcting for the pion detection efficiency, we estimate that $R(\Xi_b^0\pi^-)$ must be corrected by 1.11 ± 0.03. Slightly different-size data samples are used for the $\Xi_b(6227)^-$ and inclusive H_b^0 yield determinations, which amounts to corrections of less than 3%.

Several sources of systematic uncertainty have been considered. For the mass and width, the momentum scale uncertainty of 0.03% [43] leads to a 0.1 MeV/c^2 uncertainty on δm_K. A fit bias on the mass of 0.1 MeV/c^2 is observed in simulation, and is corrected for and a systematic uncertainty of equal size is assigned. Uncertainty due to the signal shape model is estimated by using a nonrelativistic Breit-Wigner signal shape and varying the Gaussian resolution by $\pm 10\%$ about its nominal value. With these variations, systematic uncertainties of 0.2 MeV/c^2 on δm_K, and 0.9 MeV/c^2 on $\Gamma_{\Xi_b(6227)^-}$ are obtained. Sensitivity to the background function is assessed by varying the fit range by 100 MeV/c^2 on both ends, from which maximum shifts of 0.2 MeV/c^2 in the mass and 1.6 MeV/c^2 in the width are observed; these values are assigned as systematic uncertainties. Adding these systematic uncertainties in quadrature, leads to a total systematic uncertainty of 0.3 MeV/c^2 on the mass and 1.8 MeV/c^2 on the width.

The systematic uncertainties affecting the production ratio measurements are listed in Table III. The background shape affects the yield determination, and the associated systematic uncertainty is estimated by varying the fit range as described above. (Different background models give smaller deviations.) For the signal shape, the uncertainty is dominated by the resolution function. In an alternative fit, the resolution parameters are allowed to vary within twice the expected uncertainty and we take the difference with respect to the nominal result as the uncertainty. To assess

TABLE II. Relative efficiencies ($\epsilon_{\text{rel}}^{(\prime)}$) for the SL modes. Uncertainties are due only to the finite size of the simulated samples.

Final state	7, 8 TeV	13 TeV
$\Lambda_b^0 K^-$	0.295 ± 0.006	0.305 ± 0.005
$\Xi_b^0\pi^-$	0.236 ± 0.007	0.277 ± 0.006

TABLE III. Summary of systematic uncertainties on $R(\Lambda_b^0 K^-)$ and $R(\Xi_b^0\pi^-)$, in units of 10^{-3}.

	$R(\Lambda_b^0 K^-)[10^{-3}]$		$R(\Xi_b^0\pi^-)[10^{-3}]$	
Source	7, 8 TeV	13 TeV	7, 8 TeV	13 TeV
Background shape	0.3	0.3	6.0	3.0
Signal shape	0.1	0.1	1.0	0.2
$\Xi_b(6227)^- p_{\text{T}}$	$^{+0.16}_{-0.27}$	$^{+0.14}_{-0.33}$	$^{+2.5}_{-3.2}$	$^{+0.9}_{-1.5}$
Tracking efficiency	0.03	0.03	0.5	0.2
PID requirement	0.05	0.06	0.5	0.2
$N(H_b^0)$	0.01	0.01	1.4	0.7
Simulated sample size	0.07	0.05	1.4	0.6
Total	0.4	0.4	7.0	3.3

TABLE IV. Measured ratios $R(\Lambda_b^0 K^-)$ and $R(\Xi_b^0\pi^-)$ for 7,8, and 13 TeV data, in units of 10^{-3}. The uncertainties are statistical (first) and systematic (second).

Quantity $[10^{-3}]$	7, 8 TeV	13 TeV
$R(\Lambda_b^0 K^-)$	$3.0 \pm 0.3 \pm 0.4$	$3.4 \pm 0.3 \pm 0.4$
$R(\Xi_b\pi^-)$	$47 \pm 10 \pm 7$	$22 \pm 6 \pm 3$

the dependence on the kinematical properties of the $\Xi_b(6227)^-$ resonance, the p_T spectrum in simulation is weighted by $1 \pm 0.01 \times p_T^{\Xi_b(6227)^-}/(\mathrm{GeV}/c)$, based on previous studies of the Ξ_b^0 and Λ_b^0 production spectra [44]; the relative change in efficiency is assigned as a systematic uncertainty. The charged-particle tracking efficiency, obtained using large samples of $J\psi \to \mu^+\mu^-$ decays [45], contributes an uncertainty of 1% to $\epsilon_{\mathrm{rel}}^{(\prime)}$. The systematic uncertainty of the PID requirement on the K^- or π^- from the $\Xi_b(6227)^-$ baryon is determined by comparing the PID response of kaons and pions in the $\Lambda_c^+ \to pK^-\pi^+$ decay between data and simulation, where the latter are obtained from calibration data, as described previously. The uncertainty on $N(H_b^0)$ is taken as the quadratic sum of the uncertainties on the fitted yields and the uncertainties on the $\kappa^{(\prime)}$ corrections. Lastly, the finite size of the simulated samples is taken into account.

In summary, we report the first observation of a new state, assumed to be an excited Ξ_b^- state, using pp collision data samples collected by LHCb at $\sqrt{s} = 7$, 8 and 13 TeV. The mass and width are measured to be

$$\begin{aligned} m_{\Xi_b(6227)^-} - m_{\Lambda_b^0} &= 607.3 \pm 2.0(\mathrm{stat}) \pm 0.3(\mathrm{syst})\ \mathrm{MeV}/c^2, \\ \Gamma_{\Xi_b(6227)^-} &= 18.1 \pm 5.4(\mathrm{stat}) \pm 1.8(\mathrm{syst})\ \mathrm{MeV}/c^2, \\ m_{\Xi_b(6227)^-} &= 6226.9 \pm 2.0(\mathrm{stat}) \pm 0.3(\mathrm{syst}) \\ &\quad \pm 0.2(\Lambda_b^0)\ \mathrm{MeV}/c^2, \end{aligned}$$

where for the last result we have used $m_{\Lambda_b^0} = 5619.58 \pm 0.17\ \mathrm{MeV}/c^2$ [38].

We have also measured the relative production rates to two final states, $\Lambda_b^0 K^-$ and $\Xi_b^0\pi^-$, as summarized in Table IV. The $R(\Lambda_b^0 K^-)$ values from the hadronic mode are consistent with those obtained in the SL mode, and are about an order of magnitude smaller than $R(\Xi_b^0\pi^-)$. Assuming $f_{\Xi_b^0} \simeq 0.1 f_{\Lambda_b^0}$ [46–48], we find that the ratio of branching fractions $\mathcal{B}(\Xi_b(6227)^- \to \Lambda_b^0 K^-)/\mathcal{B}(\Xi_b(6227)^- \to \Xi_b^0\pi^-) \simeq 1$, albeit with sizable uncertainty ($\approx \pm 0.5$) due to theoretical assumptions and the values of experimental inputs.

The mass of this structure and the observed decay modes are consistent with expectations of either a $\Xi_b(1P)^-$ or $\Xi_b(2S)^-$ state [8–23]. As there are several excited Ξ_b^- states expected in this mass region, the presence of more than one of these states contributing to this peak cannot be excluded. More precise measurements of the width and the relative branching fractions to $\Lambda_b^0 K^-$ and $\Xi_b^0\pi^-$, as well as $\Xi_b'\pi^-$ and $\Xi_b{}^*\pi^-$, could help to determine the J^P quantum numbers of this state [20].

We express our gratitude to our colleagues in the CERN accelerator departments for the excellent performance of the LHC. We thank the technical and administrative staff at the LHCb institutes. We acknowledge support from CERN and from the national agencies: CAPES, CNPq, FAPERJ and FINEP (Brazil); MOST and NSFC (China); CNRS/IN2P3 (France); BMBF, DFG and MPG (Germany); INFN (Italy); NWO (The Netherlands); MNiSW and NCN (Poland); MEN/IFA (Romania); MinES and FASO (Russia); Generalitat Valenciana and MinECo (Spain); SNSF and SER (Switzerland); NASU (Ukraine); STFC (United Kingdom); NSF (USA). We acknowledge the computing resources that are provided by CERN, IN2P3 (France), KIT and DESY (Germany), INFN (Italy), SURF (The Netherlands), PIC (Spain), GridPP (United Kingdom), RRCKI and Yandex LLC (Russia), CSCS (Switzerland), IFIN-HH (Romania), CBPF (Brazil), PL-GRID (Poland) and OSC (USA). We are indebted to the communities behind the multiple open-source software packages on which we depend. Individual groups or members have received support from AvH Foundation (Germany), EPLANET, Marie Skłodowska-Curie Actions and ERC (European Union), ANR, Labex P2IO and OCEVU, and Région Auvergne-Rhône-Alpes (France), Key Research Program of Frontier Sciences of CAS, CAS PIFI, and the Thousand Talents Program (China), RFBR, RSF and Yandex LLC (Russia), GVA, XuntaGal and GENCAT (Spain), Herchel Smith Fund, the Royal Society, the English-Speaking Union and the Leverhulme Trust (United Kingdom).

[1] M. Gell-Mann, A schematic model of baryons and mesons, Phys. Lett. **8**, 214 (1964).
[2] G. Zweig, An SU_3 model for strong interaction symmetry and its breaking, CERN-TH-412, reprinted in *Developments in the Quark Theory of Hadrons* 1, 22 (1980), edited by D. Lichtenberg and S. Rosen (Hadronic Press, Nonantum, 1980).
[3] E. Klempt and J.-M. Richard, Baryon spectroscopy, Rev. Mod. Phys. **82**, 1095 (2010).
[4] D. Ebert, T. Feldmann, C. Kettner, and H. Reinhardt, A diquark model for baryons containing one heavy quark, Z. Phys. C **71**, 329 (1996).
[5] R. Aaij *et al.* (LHCb Collaboration), Observation of Two New Ξ_b^- Baryon Resonances, Phys. Rev. Lett. **114**, 062004 (2015).
[6] S. Chatrchyan *et al.* (CMS Collaboration), Observation of a New Ξ_b Baryon, Phys. Rev. Lett. **108**, 252002 (2012).
[7] R. Aaij *et al.* (LHCb Collaboration), Measurement of the properties of the $\Xi_b{}^{*0}$ baryon, J. High Energy Phys. 05 (2016) 161.

[8] D. Ebert, R. N. Faustov, and V. O. Galkin, Spectroscopy and Regge trajectories of heavy baryons in the relativistic quark-diquark picture, Phys. Rev. D **84**, 014025 (2011).

[9] D. Ebert, R. N. Faustov, and V. O. Galkin, Masses of excited heavy baryons in the relativistic quark-diquark picture, Phys. Lett. B **659**, 612 (2008).

[10] W. Roberts and M. Pervin, Heavy baryons in a quark model, Int. J. Mod. Phys. A **23**, 2817 (2008).

[11] H. Garcilazo, J. Vijande, and A. Valcarce, Faddeev study of heavy-baryon spectroscopy, J. Phys. G **34**, 961 (2007).

[12] B. Chen, K.-W. Wei, and A. Zhang, Investigation of Λ_Q and Ξ_Q baryons in the heavy quark-light diquark picture, Eur. Phys. J. A **51**, 82 (2015).

[13] Q. Mao, H. X. Chen, W. Chen, A. Hosaka, X. Liu, and S. L. Zhu, QCD sum rule calculation for P-wave bottom baryons, Phys. Rev. D **92**, 114007 (2015).

[14] I. L. Grach, I. M. Narodetskii, M. A. Trusov, and A. I. Veselov, Heavy baryon spectroscopy in the QCD string model, in *Particles and Nuclei. Proceedings of the 18th International Conference, PANIC08, Eilat, Israel, 2008*, arXiv:0811.2184.

[15] C. Garcia-Recio, J. Nieves, O. Romanets, L. L. Salcedo, and L. Tolos, Odd parity bottom-flavored baryon resonances, Phys. Rev. D **87**, 034032 (2013).

[16] M. Karliner, B. Keren-Zur, H. J. Lipkin, and J. L. Rosner, The quark model and b baryons, Ann. Phys. (Amsterdam) **324**, 2 (2009).

[17] Z.-G. Wang, Analysis of the $1/2^-$ and $3/2^-$ heavy and doubly heavy baryon states with QCD sum rules, Eur. Phys. J. A **47**, 81 (2011).

[18] A. Valcarce, H. Garcilazo, and J. Vijande, Towards an understanding of heavy baryon spectroscopy, Eur. Phys. J. A **37**, 217 (2008).

[19] J. Vijande, A. Valcarce, T. F. Carames, and H. Garcilazo, Heavy hadron spectroscopy: A quark model perspective, Int. J. Mod. Phys. E **22**, 1330011 (2013).

[20] K.-L. Wang, Y.-X. Yao, X.-H. Zhong, and Q. Zhao, Strong and radiative decays of the low-lying S- and P-wave singly heavy baryons, Phys. Rev. D **96**, 116016 (2017).

[21] Z.-Y. Wang, J.-J. Qi, X.-H. Guo, and K.-W. Wei, Spectra of charmed and bottom baryons with hyperfine interaction, Chin. Phys. C **41**, 093103 (2017).

[22] H.-X. Chen, Q. Mao, A. Hosaka, X. Liu, and S. L. Zhu, D-wave charmed and bottomed baryons from QCD sum rules, Phys. Rev. D **94**, 114016 (2016).

[23] K. Thakkar, Z. Shah, A. K. Rai, and P. C. Vinodkumar, Excited state mass spectra and Regge trajectories of bottom baryons, Nucl. Phys. **A965**, 57 (2017).

[24] R. Aaij *et al.* (LHCb Collaboration), Observation of Excited Λ_b^0 Baryons, Phys. Rev. Lett. **109**, 172003 (2012).

[25] A. A. Alves Jr. *et al.* (LHCb Collaboration), The LHCb detector at the LHC, J. Instrum. **3**, S08005 (2008).

[26] R. Aaij *et al.* (LHCb Collaboration), LHCb detector performance, Int. J. Mod. Phys. A **30**, 1530022 (2015).

[27] R. Aaij *et al.* (LHCb Collaboration), The LHCb trigger and its performance in 2011, J. Instrum. **8**, P04022 (2013).

[28] V. V. Gligorov and M. Williams, Efficient, reliable and fast high-level triggering using a bonsai boosted decision tree, J. Instrum. **8**, P02013 (2013).

[29] T. Sjöstrand, S. Mrenna, and P. Skands, A brief introduction to PYTHIA 8.1, Comput. Phys. Commun. **178**, 852 (2008).

[30] T. Sjöstrand, S. Mrenna, and P. Skands, PYTHIA 6.4 physics and manual, J. High Energy Phys. 05 (2006) 026.

[31] I. Belyaev *et al.*, Handling of the generation of primary events in Gauss, the LHCb simulation framework, J. Phys. Conf. Ser. **331**, 032047 (2011).

[32] D. J. Lange, The EvtGen particle decay simulation package, Nucl. Instrum. Methods Phys. Res., Sect. A **462**, 152 (2001).

[33] P. Golonka and Z. Was, PHOTOS Monte Carlo: A precision tool for QED corrections in Z and W decays, Eur. Phys. J. C **45**, 97 (2006).

[34] J. Allison *et al.* (Geant4 Collaboration), Geant4 developments and applications, IEEE Trans. Nucl. Sci. **53**, 270 (2006); S. Agostinelli *et al.* (Geant4 Collaboration), Geant4: A simulation toolkit, Nucl. Instrum. Methods Phys. Res., Sect. A **506**, 250 (2003).

[35] M. Clemencic, G. Corti, S. Easo, C. R. Jones, S. Miglioranzi, M. Pappagallo, and P. Robbe, The LHCb simulation application, Gauss: Design, evolution and experience, J. Phys. Conf. Ser. **331**, 032023 (2011).

[36] B. P. Roe, H.-J. Yang, J. Zhu, Y. Liu, I. Stancu, and G. McGregor, Boosted decision trees as an alternative to artificial neural networks for particle identification, Nucl. Instrum. Methods Phys. Res., Sect. A **543**, 577 (2005).

[37] Y. Freund and R. E. Schapire, A decision-theoretic generalization of on-line learning and an application to boosting, J. Comput. Syst. Sci. **55**, 119 (1997).

[38] C. Patrignani *et al.* (Particle Data Group), Review of particle physics, Chin. Phys. C **40**, 100001 (2016), and 2017 update.

[39] See Supplemental Material at http://link.aps.org/supplemental/10.1103/PhysRevLett.121.072002 for the mass resolution functions on δm_K and δm_π.

[40] J. D. Jackson, Remarks on the phenomenological analysis of resonances, Nuovo Cimento **34**, 1644 (1964).

[41] J. Blatt and V. Weisskopf, *Theoretical Nuclear Physics* (John Wiley & Sons, New York, 1952).

[42] R. Brun and F. Rademakers, ROOT: An object oriented data analysis framework, Nucl. Instrum. Methods Phys. Res., Sect. A **389**, 81 (1997); the threshold function is described by the `RooDstD0Bg` class within ROOT.

[43] R. Aaij *et al.* (LHCb Collaboration), Precision measurement of D meson mass differences, J. High Energy Phys. 06 (2013) 065.

[44] R. Aaij *et al.* (LHCb Collaboration), Precision Measurement of the Mass and Lifetime of the Ξ_b^0 Baryon, Phys. Rev. Lett. **113**, 032001 (2014).

[45] R. Aaij *et al.* (LHCb Collaboration), Measurement of the track reconstruction efficiency at LHCb, J. Instrum. **10**, P02007 (2015).

[46] M. Voloshin, Remarks on the measurement of the decay $\Xi_b^- \to \Lambda_b^0 \pi^-$, arXiv:1510.05568.

[47] Y. K. Hsiao, P. Y. Lin, L. W. Luo, and C. Q. Geng, Fragmentation fractions of two-body b-baryon decays, Phys. Lett. B **751**, 127 (2015).

[48] H.-Y. Jiang and F.-S. Yu, Fragmentation-fraction ratio f_{Ξ_b}/f_{Λ_b} in b- and c-baryon decays, Eur. Phys. J. C **78**, 224 (2018).

R. Aaij,[27] B. Adeva,[41] M. Adinolfi,[48] C. A. Aidala,[73] Z. Ajaltouni,[5] S. Akar,[59] P. Albicocco,[18] J. Albrecht,[10] F. Alessio,[42] M. Alexander,[53] A. Alfonso Albero,[40] S. Ali,[27] G. Alkhazov,[33] P. Alvarez Cartelle,[55] A. A. Alves Jr,[59] S. Amato,[2] S. Amerio,[23] Y. Amhis,[7] L. An,[3] L. Anderlini,[17] G. Andreassi,[43] M. Andreotti,[16,a] J. E. Andrews,[60] R. B. Appleby,[56] F. Archilli,[27] P. d'Argent,[12] J. Arnau Romeu,[6] A. Artamonov,[39] M. Artuso,[61] K. Arzymatov,[37] E. Aslanides,[6] M. Atzeni,[44] S. Bachmann,[12] J. J. Back,[50] S. Baker,[55] V. Balagura,[7,b] W. Baldini,[16] A. Baranov,[37] R. J. Barlow,[56] S. Barsuk,[7] W. Barter,[56] F. Baryshnikov,[34] V. Batozskaya,[31] B. Batsukh,[61] V. Battista,[43] A. Bay,[43] J. Beddow,[53] F. Bedeschi,[24] I. Bediaga,[1] A. Beiter,[61] L. J. Bel,[27] N. Beliy,[63] V. Bellee,[43] N. Belloli,[20,c] K. Belous,[39] I. Belyaev,[34,42] E. Ben-Haim,[8] G. Bencivenni,[18] S. Benson,[27] S. Beranek,[9] A. Berezhnoy,[35] R. Bernet,[44] D. Berninghoff,[12] E. Bertholet,[8] A. Bertolin,[23] C. Betancourt,[44] F. Betti,[15,42] M. O. Bettler,[49] M. van Beuzekom,[27] Ia. Bezshyiko,[44] L. Bian,[64] S. Bifani,[47] P. Billoir,[8] A. Birnkraut,[10] A. Bizzeti,[17,d] M. Bjørn,[57] T. Blake,[50] F. Blanc,[43] S. Blusk,[61] D. Bobulska,[53] V. Bocci,[26] O. Boente Garcia,[41] T. Boettcher,[58] A. Bondar,[38,e] N. Bondar,[33] S. Borghi,[56,42] M. Borisyak,[37] M. Borsato,[41,42] F. Bossu,[7] M. Boubdir,[9] T. J. V. Bowcock,[54] C. Bozzi,[16,42] S. Braun,[12] M. Brodski,[42] J. Brodzicka,[29] D. Brundu,[22] E. Buchanan,[48] A. Buonaura,[44] C. Burr,[56] A. Bursche,[22] J. Buytaert,[42] W. Byczynski,[42] S. Cadeddu,[22] H. Cai,[64] R. Calabrese,[16,a] R. Calladine,[47] M. Calvi,[20,c] M. Calvo Gomez,[40,f] A. Camboni,[40,f] P. Campana,[18] D. H. Campora Perez,[42] L. Capriotti,[56] A. Carbone,[15,g] G. Carboni,[25] R. Cardinale,[19,h] A. Cardini,[22] P. Carniti,[20,c] L. Carson,[52] K. Carvalho Akiba,[2] G. Casse,[54] L. Cassina,[20] M. Cattaneo,[42] G. Cavallero,[19,h] R. Cenci,[24,i] D. Chamont,[7] M. G. Chapman,[48] M. Charles,[8] Ph. Charpentier,[42] G. Chatzikonstantinidis,[47] M. Chefdeville,[4] V. Chekalina,[37] C. Chen,[3] S. Chen,[22] S.-G. Chitic,[42] V. Chobanova,[41] M. Chrzaszcz,[42] A. Chubykin,[33] P. Ciambrone,[18] X. Cid Vidal,[41] G. Ciezarek,[42] P. E. L. Clarke,[52] M. Clemencic,[42] H. V. Cliff,[49] J. Closier,[42] V. Coco,[42] J. Cogan,[6] E. Cogneras,[5] L. Cojocariu,[32] P. Collins,[42] T. Colombo,[42] A. Comerma-Montells,[12] A. Contu,[22] G. Coombs,[42] S. Coquereau,[40] G. Corti,[42] M. Corvo,[16,a] C. M. Costa Sobral,[50] B. Couturier,[42] G. A. Cowan,[52] D. C. Craik,[58] A. Crocombe,[50] M. Cruz Torres,[1] R. Currie,[52] C. D'Ambrosio,[42] F. Da Cunha Marinho,[2] C. L. Da Silva,[74] E. Dall'Occo,[27] J. Dalseno,[48] A. Danilina,[34] A. Davis,[3] O. De Aguiar Francisco,[42] K. De Bruyn,[42] S. De Capua,[56] M. De Cian,[43] J. M. De Miranda,[1] L. De Paula,[2] M. De Serio,[14,j] P. De Simone,[18] C. T. Dean,[53] D. Decamp,[4] L. Del Buono,[8] B. Delaney,[49] H.-P. Dembinski,[11] M. Demmer,[10] A. Dendek,[30] D. Derkach,[37] O. Deschamps,[5] F. Dettori,[54] B. Dey,[65] A. Di Canto,[42] P. Di Nezza,[18] S. Didenko,[70] H. Dijkstra,[42] F. Dordei,[42] M. Dorigo,[42,k] A. Dosil Suárez,[41] L. Douglas,[53] A. Dovbnya,[45] K. Dreimanis,[54] L. Dufour,[27] G. Dujany,[8] P. Durante,[42] J. M. Durham,[74] D. Dutta,[56] R. Dzhelyadin,[39] M. Dziewiecki,[12] A. Dziurda,[42] A. Dzyuba,[33] S. Easo,[51] U. Egede,[55] V. Egorychev,[34] S. Eidelman,[38,e] S. Eisenhardt,[52] U. Eitschberger,[10] R. Ekelhof,[10] L. Eklund,[53] S. Ely,[61] A. Ene,[32] S. Escher,[9] S. Esen,[27] H. M. Evans,[49] T. Evans,[57] A. Falabella,[15] N. Farley,[47] S. Farry,[54] D. Fazzini,[20,42,c] L. Federici,[25] G. Fernandez,[40] P. Fernandez Declara,[42] A. Fernandez Prieto,[41] F. Ferrari,[15] L. Ferreira Lopes,[43] F. Ferreira Rodrigues,[2] M. Ferro-Luzzi,[42] S. Filippov,[36] R. A. Fini,[14] M. Fiorini,[16,a] M. Firlej,[30] C. Fitzpatrick,[43] T. Fiutowski,[30] F. Fleuret,[7,b] M. Fontana,[22,42] F. Fontanelli,[19,h] R. Forty,[42] V. Franco Lima,[54] M. Frank,[42] C. Frei,[42] J. Fu,[21,l] W. Funk,[42] C. Färber,[42] M. Féo Pereira Rivello Carvalho,[27] E. Gabriel,[52] A. Gallas Torreira,[41] D. Galli,[15,g] S. Gallorini,[23] S. Gambetta,[52] M. Gandelman,[2] P. Gandini,[21] Y. Gao,[3] L. M. Garcia Martin,[72] B. Garcia Plana,[41] J. García Pardiñas,[44] J. Garra Tico,[49] L. Garrido,[40] D. Gascon,[40] C. Gaspar,[42] L. Gavardi,[10] G. Gazzoni,[5] D. Gerick,[12] E. Gersabeck,[56] M. Gersabeck,[56] T. Gershon,[50] Ph. Ghez,[4] S. Gianì,[43] V. Gibson,[49] O. G. Girard,[43] L. Giubega,[32] K. Gizdov,[52] V. V. Gligorov,[8] D. Golubkov,[34] A. Golutvin,[55,70] A. Gomes,[1,m] I. V. Gorelov,[35] C. Gotti,[20,c] E. Govorkova,[27] J. P. Grabowski,[12] R. Graciani Diaz,[40] L. A. Granado Cardoso,[42] E. Graugés,[40] E. Graverini,[44] G. Graziani,[17] A. Grecu,[32] R. Greim,[27] P. Griffith,[22] L. Grillo,[56] L. Gruber,[42] B. R. Gruberg Cazon,[57] O. Grünberg,[67] C. Gu,[3] E. Gushchin,[36] Yu. Guz,[39,42] T. Gys,[42] C. Göbel,[62] T. Hadavizadeh,[57] C. Hadjivasiliou,[5] G. Haefeli,[43] C. Haen,[42] S. C. Haines,[49] B. Hamilton,[60] X. Han,[12] T. H. Hancock,[57] S. Hansmann-Menzemer,[12] N. Harnew,[57] S. T. Harnew,[48] C. Hasse,[42] M. Hatch,[42] J. He,[63] M. Hecker,[55] K. Heinicke,[10] A. Heister,[9] K. Hennessy,[54] L. Henry,[72] E. van Herwijnen,[42] M. Heß,[67] A. Hicheur,[2]

D. Hill,[57] M. Hilton,[56] P. H. Hopchev,[43] W. Hu,[65] W. Huang,[63] Z. C. Huard,[59] W. Hulsbergen,[27] T. Humair,[55] M. Hushchyn,[37] D. Hutchcroft,[54] P. Ibis,[10] M. Idzik,[30] P. Ilten,[47] K. Ivshin,[33] R. Jacobsson,[42] J. Jalocha,[57] E. Jans,[27] A. Jawahery,[60] F. Jiang,[3] M. John,[57] D. Johnson,[42] C. R. Jones,[49] C. Joram,[42] B. Jost,[42] N. Jurik,[57] S. Kandybei,[45] M. Karacson,[42] J. M. Kariuki,[48] S. Karodia,[53] N. Kazeev,[37] M. Kecke,[12] F. Keizer,[49] M. Kelsey,[61] M. Kenzie,[49] T. Ketel,[28] E. Khairullin,[37] B. Khanji,[12] C. Khurewathanakul,[43] K. E. Kim,[61] T. Kirn,[9] S. Klaver,[18] K. Klimaszewski,[31] T. Klimkovich,[11] S. Koliiev,[46] M. Kolpin,[12] R. Kopecna,[12] P. Koppenburg,[27] S. Kotriakhova,[33] M. Kozeiha,[5] L. Kravchuk,[36] M. Kreps,[50] F. Kress,[55] P. Krokovny,[38,e] W. Krupa,[30] W. Krzemien,[31] W. Kucewicz,[29,n] M. Kucharczyk,[29] V. Kudryavtsev,[38,e] A. K. Kuonen,[43] T. Kvaratskheliya,[34,42] D. Lacarrere,[42] G. Lafferty,[56] A. Lai,[22] D. Lancierini,[44] G. Lanfranchi,[18] C. Langenbruch,[9] T. Latham,[50] C. Lazzeroni,[47] R. Le Gac,[6] A. Leflat,[35] J. Lefrançois,[7] R. Lefèvre,[5] F. Lemaitre,[42] O. Leroy,[6] T. Lesiak,[29] B. Leverington,[12] P.-R. Li,[63] T. Li,[3] Z. Li,[61] X. Liang,[61] T. Likhomanenko,[69] R. Lindner,[42] F. Lionetto,[44] V. Lisovskyi,[7] X. Liu,[3] D. Loh,[50] A. Loi,[22] I. Longstaff,[53] J. H. Lopes,[2] D. Lucchesi,[23,o] M. Lucio Martinez,[41] A. Lupato,[23] E. Luppi,[16,a] O. Lupton,[42] A. Lusiani,[24] X. Lyu,[63] F. Machefert,[7] F. Maciuc,[32] V. Macko,[43] P. Mackowiak,[10] S. Maddrell-Mander,[48] O. Maev,[33,42] K. Maguire,[56] D. Maisuzenko,[33] M. W. Majewski,[30] S. Malde,[57] B. Malecki,[29] A. Malinin,[69] T. Maltsev,[38,e] G. Manca,[22,p] G. Mancinelli,[6] D. Marangotto,[21,l] J. Maratas,[5,q] J. F. Marchand,[4] U. Marconi,[15] C. Marin Benito,[40] M. Marinangeli,[43] P. Marino,[43] J. Marks,[12] G. Martellotti,[26] M. Martin,[6] M. Martinelli,[43] D. Martinez Santos,[41] F. Martinez Vidal,[72] A. Massafferri,[1] R. Matev,[42] A. Mathad,[50] Z. Mathe,[42] C. Matteuzzi,[20] A. Mauri,[44] E. Maurice,[7,b] B. Maurin,[43] A. Mazurov,[47] M. McCann,[55,42] A. McNab,[56] R. McNulty,[13] J. V. Mead,[54] B. Meadows,[59] C. Meaux,[6] F. Meier,[10] N. Meinert,[67] D. Melnychuk,[31] M. Merk,[27] A. Merli,[21,l] E. Michielin,[23] D. A. Milanes,[66] E. Millard,[50] M.-N. Minard,[4] L. Minzoni,[16,a] D. S. Mitzel,[12] A. Mogini,[8] J. Molina Rodriguez,[1,r] T. Mombächer,[10] I. A. Monroy,[66] S. Monteil,[5] M. Morandin,[23] G. Morello,[18] M. J. Morello,[24,s] O. Morgunova,[69] J. Moron,[30] A. B. Morris,[6] R. Mountain,[61] F. Muheim,[52] M. Mulder,[27] D. Müller,[42] J. Müller,[10] K. Müller,[44] V. Müller,[10] P. Naik,[48] T. Nakada,[43] R. Nandakumar,[51] A. Nandi,[57] T. Nanut,[43] I. Nasteva,[2] M. Needham,[52] N. Neri,[21] S. Neubert,[12] N. Neufeld,[42] M. Neuner,[12] T. D. Nguyen,[43] C. Nguyen-Mau,[43,t] S. Nieswand,[9] R. Niet,[10] N. Nikitin,[35] A. Nogay,[69] D. P. O'Hanlon,[15] A. Oblakowska-Mucha,[30] V. Obraztsov,[39] S. Ogilvy,[18] R. Oldeman,[22,p] C. J. G. Onderwater,[68] A. Ossowska,[29] J. M. Otalora Goicochea,[2] P. Owen,[44] A. Oyanguren,[72] P. R. Pais,[43] A. Palano,[14] M. Palutan,[18,42] G. Panshin,[71] A. Papanestis,[51] M. Pappagallo,[52] L. L. Pappalardo,[16,a] W. Parker,[60] C. Parkes,[56] G. Passaleva,[17,42] A. Pastore,[14] M. Patel,[55] C. Patrignani,[15,g] A. Pearce,[42] A. Pellegrino,[27] G. Penso,[26] M. Pepe Altarelli,[42] S. Perazzini,[42] D. Pereima,[34] P. Perret,[5] L. Pescatore,[43] K. Petridis,[48] A. Petrolini,[19,h] A. Petrov,[69] M. Petruzzo,[21,l] B. Pietrzyk,[4] G. Pietrzyk,[43] M. Pikies,[29] D. Pinci,[26] J. Pinzino,[42] F. Pisani,[42] A. Pistone,[19,h] A. Piucci,[12] V. Placinta,[32] S. Playfer,[52] J. Plews,[47] M. Plo Casasus,[41] F. Polci,[8] M. Poli Lener,[18] A. Poluektov,[50] N. Polukhina,[70,u] I. Polyakov,[61] E. Polycarpo,[2] G. J. Pomery,[48] S. Ponce,[42] A. Popov,[39] D. Popov,[47,11] S. Poslavskii,[39] C. Potterat,[2] E. Price,[48] J. Prisciandaro,[41] C. Prouve,[48] V. Pugatch,[46] A. Puig Navarro,[44] H. Pullen,[57] G. Punzi,[24,i] W. Qian,[63] J. Qin,[63] R. Quagliani,[8] B. Quintana,[5] B. Rachwal,[30] J. H. Rademacker,[48] M. Rama,[24] M. Ramos Pernas,[41] M. S. Rangel,[2] F. Ratnikov,[37,v] G. Raven,[28] M. Ravonel Salzgeber,[42] M. Reboud,[4] F. Redi,[43] S. Reichert,[10] A. C. dos Reis,[1] F. Reiss,[8] C. Remon Alepuz,[72] Z. Ren,[3] V. Renaudin,[7] S. Ricciardi,[51] S. Richards,[48] K. Rinnert,[54] P. Robbe,[7] A. Robert,[8] A. B. Rodrigues,[43] E. Rodrigues,[59] J. A. Rodriguez Lopez,[66] A. Rogozhnikov,[37] S. Roiser,[42] A. Rollings,[57] V. Romanovskiy,[39] A. Romero Vidal,[41] M. Rotondo,[18] M. S. Rudolph,[61] T. Ruf,[42] J. Ruiz Vidal,[72] J. J. Saborido Silva,[41] N. Sagidova,[33] B. Saitta,[22,p] V. Salustino Guimaraes,[62] C. Sanchez Gras,[27] C. Sanchez Mayordomo,[72] B. Sanmartin Sedes,[41] R. Santacesaria,[26] C. Santamarina Rios,[41] M. Santimaria,[18] E. Santovetti,[25,w] G. Sarpis,[56] A. Sarti,[18,x] C. Satriano,[26,y] A. Satta,[25] M. Saur,[63] D. Savrina,[34,35] S. Schael,[9] M. Schellenberg,[10] M. Schiller,[53] H. Schindler,[42] M. Schmelling,[11] T. Schmelzer,[10] B. Schmidt,[42] O. Schneider,[43] A. Schopper,[42] H. F. Schreiner,[59] M. Schubiger,[43] M. H. Schune,[7] R. Schwemmer,[42] B. Sciascia,[18] A. Sciubba,[26,x] A. Semennikov,[34] E. S. Sepulveda,[8] A. Sergi,[47,42] N. Serra,[44] J. Serrano,[6] L. Sestini,[23] P. Seyfert,[42] M. Shapkin,[39] Y. Shcheglov,[33†] T. Shears,[54] L. Shekhtman,[38,e] V. Shevchenko,[69] E. Shmanin,[70] B. G. Siddi,[16] R. Silva Coutinho,[44] L. Silva de Oliveira,[2] G. Simi,[23,o] S. Simone,[14,j] N. Skidmore,[12] T. Skwarnicki,[61] E. Smith,[9] I. T. Smith,[52] M. Smith,[55] M. Soares,[15] l. Soares Lavra,[1] M. D. Sokoloff,[59] F. J. P. Soler,[53] B. Souza De Paula,[2] B. Spaan,[10] P. Spradlin,[53] F. Stagni,[42] M. Stahl,[12] S. Stahl,[42] P. Stefko,[43] S. Stefkova,[55] O. Steinkamp,[44] S. Stemmle,[12] O. Stenyakin,[39] M. Stepanova,[33] H. Stevens,[10] S. Stone,[61] B. Storaci,[44] S. Stracka,[24,i] M. E. Stramaglia,[43] M. Straticiuc,[32] U. Straumann,[44] S. Strokov,[71] J. Sun,[3] L. Sun,[64] K. Swientek,[30] V. Syropoulos,[28] T. Szumlak,[30] M. Szymanski,[63] S. T'Jampens,[4] Z. Tang,[3] A. Tayduganov,[6] T. Tekampe,[10] G. Tellarini,[16] F. Teubert,[42] E. Thomas,[42] J. van Tilburg,[27] M. J. Tilley,[55] V. Tisserand,[5] M. Tobin,[43] S. Tolk,[42] L. Tomassetti,[16,a] D. Tonelli,[24] D. Y. Tou,[8] R. Tourinho Jadallah Aoude,[1] E. Tournefier,[4] M. Traill,[53]

M. T. Tran,[43] A. Trisovic,[49] A. Tsaregorodtsev,[6] A. Tully,[49] N. Tuning,[27,42] A. Ukleja,[31] A. Usachov,[7] A. Ustyuzhanin,[37] U. Uwer,[12] C. Vacca,[22,p] A. Vagner,[71] V. Vagnoni,[15] A. Valassi,[42] S. Valat,[42] G. Valenti,[15] R. Vazquez Gomez,[42] P. Vazquez Regueiro,[41] S. Vecchi,[16] M. van Veghel,[27] J. J. Velthuis,[48] M. Veltri,[17,z] G. Veneziano,[57] A. Venkateswaran,[61] T. A. Verlage,[9] M. Vernet,[5] M. Vesterinen,[57] J. V. Viana Barbosa,[42] D. Vieira,[63] M. Vieites Diaz,[41] H. Viemann,[67] X. Vilasis-Cardona,[40,f] A. Vitkovskiy,[27] M. Vitti,[49] V. Volkov,[35] A. Vollhardt,[44] B. Voneki,[42] A. Vorobyev,[33] V. Vorobyev,[38,e] C. Voß,[9] J. A. de Vries,[27] C. Vázquez Sierra,[27] R. Waldi,[67] J. Walsh,[24] J. Wang,[61] M. Wang,[3] Y. Wang,[65] Z. Wang,[44] D. R. Ward,[49] H. M. Wark,[54] N. K. Watson,[47] D. Websdale,[55] A. Weiden,[44] C. Weisser,[58] M. Whitehead,[9] J. Wicht,[50] G. Wilkinson,[57] M. Wilkinson,[61] M. R. J. Williams,[56] M. Williams,[58] T. Williams,[47] F. F. Wilson,[51,42] J. Wimberley,[60] M. Winn,[7] J. Wishahi,[10] W. Wislicki,[31] M. Witek,[29] G. Wormser,[7] S. A. Wotton,[49] K. Wyllie,[42] D. Xiao,[65] Y. Xie,[65] A. Xu,[3] M. Xu,[65] Q. Xu,[63] Z. Xu,[3] Z. Xu,[4] Z. Yang,[3] Z. Yang,[60] Y. Yao,[61] H. Yin,[65] J. Yu,[65,aa] X. Yuan,[61] O. Yushchenko,[39] K. A. Zarebski,[47] M. Zavertyaev,[11,u] D. Zhang,[65] L. Zhang,[3] W. C. Zhang,[3,bb] Y. Zhang,[7] A. Zhelezov,[12] Y. Zheng,[63] X. Zhu,[3] V. Zhukov,[9,35] J. B. Zonneveld,[52] and S. Zucchelli[15]

(LHCb Collaboration)

[1]*Centro Brasileiro de Pesquisas Físicas (CBPF), Rio de Janeiro, Brazil*
[2]*Universidade Federal do Rio de Janeiro (UFRJ), Rio de Janeiro, Brazil*
[3]*Center for High Energy Physics, Tsinghua University, Beijing, China*
[4]*Univ. Grenoble Alpes, Univ. Savoie Mont Blanc, CNRS, IN2P3-LAPP, Annecy, France*
[5]*Clermont Université, Université Blaise Pascal, CNRS/IN2P3, LPC, Clermont-Ferrand, France*
[6]*Aix Marseille Univ, CNRS/IN2P3, CPPM, Marseille, France*
[7]*LAL, Univ. Paris-Sud, CNRS/IN2P3, Université Paris-Saclay, Orsay, France*
[8]*LPNHE, Université Pierre et Marie Curie, Université Paris Diderot, CNRS/IN2P3, Paris, France*
[9]*I. Physikalisches Institut, RWTH Aachen University, Aachen, Germany*
[10]*Fakultät Physik, Technische Universität Dortmund, Dortmund, Germany*
[11]*Max-Planck-Institut für Kernphysik (MPIK), Heidelberg, Germany*
[12]*Physikalisches Institut, Ruprecht-Karls-Universität Heidelberg, Heidelberg, Germany*
[13]*School of Physics, University College Dublin, Dublin, Ireland*
[14]*INFN Sezione di Bari, Bari, Italy*
[15]*INFN Sezione di Bologna, Bologna, Italy*
[16]*INFN Sezione di Ferrara, Ferrara, Italy*
[17]*INFN Sezione di Firenze, Firenze, Italy*
[18]*INFN Laboratori Nazionali di Frascati, Frascati, Italy*
[19]*INFN Sezione di Genova, Genova, Italy*
[20]*INFN Sezione di Milano-Bicocca, Milano, Italy*
[21]*INFN Sezione di Milano, Milano, Italy*
[22]*INFN Sezione di Cagliari, Monserrato, Italy*
[23]*INFN Sezione di Padova, Padova, Italy*
[24]*INFN Sezione di Pisa, Pisa, Italy*
[25]*INFN Sezione di Roma Tor Vergata, Roma, Italy*
[26]*INFN Sezione di Roma La Sapienza, Roma, Italy*
[27]*Nikhef National Institute for Subatomic Physics, Amsterdam, Netherlands*
[28]*Nikhef National Institute for Subatomic Physics and VU University Amsterdam, Amsterdam, Netherlands*
[29]*Henryk Niewodniczanski Institute of Nuclear Physics Polish Academy of Sciences, Kraków, Poland*
[30]*AGH—University of Science and Technology, Faculty of Physics and Applied Computer Science, Kraków, Poland*
[31]*National Center for Nuclear Research (NCBJ), Warsaw, Poland*
[32]*Horia Hulubei National Institute of Physics and Nuclear Engineering, Bucharest-Magurele, Romania*
[33]*Petersburg Nuclear Physics Institute (PNPI), Gatchina, Russia*
[34]*Institute of Theoretical and Experimental Physics (ITEP), Moscow, Russia*
[35]*Institute of Nuclear Physics, Moscow State University (SINP MSU), Moscow, Russia*
[36]*Institute for Nuclear Research of the Russian Academy of Sciences (INR RAS), Moscow, Russia*
[37]*Yandex School of Data Analysis, Moscow, Russia*
[38]*Budker Institute of Nuclear Physics (SB RAS), Novosibirsk, Russia*
[39]*Institute for High Energy Physics (IHEP), Protvino, Russia*
[40]*ICCUB, Universitat de Barcelona, Barcelona, Spain*
[41]*Instituto Galego de Física de Altas Enerxías (IGFAE), Universidade de Santiago de Compostela, Santiago de Compostela, Spain*

[42]European Organization for Nuclear Research (CERN), Geneva, Switzerland
[43]Institute of Physics, Ecole Polytechnique Fédérale de Lausanne (EPFL), Lausanne, Switzerland
[44]Physik-Institut, Universität Zürich, Zürich, Switzerland
[45]NSC Kharkiv Institute of Physics and Technology (NSC KIPT), Kharkiv, Ukraine
[46]Institute for Nuclear Research of the National Academy of Sciences (KINR), Kyiv, Ukraine
[47]University of Birmingham, Birmingham, United Kingdom
[48]H.H. Wills Physics Laboratory, University of Bristol, Bristol, United Kingdom
[49]Cavendish Laboratory, University of Cambridge, Cambridge, United Kingdom
[50]Department of Physics, University of Warwick, Coventry, United Kingdom
[51]STFC Rutherford Appleton Laboratory, Didcot, United Kingdom
[52]School of Physics and Astronomy, University of Edinburgh, Edinburgh, United Kingdom
[53]School of Physics and Astronomy, University of Glasgow, Glasgow, United Kingdom
[54]Oliver Lodge Laboratory, University of Liverpool, Liverpool, United Kingdom
[55]Imperial College London, London, United Kingdom
[56]School of Physics and Astronomy, University of Manchester, Manchester, United Kingdom
[57]Department of Physics, University of Oxford, Oxford, United Kingdom
[58]Massachusetts Institute of Technology, Cambridge, Massachusetts, USA
[59]University of Cincinnati, Cincinnati, Ohio, USA
[60]University of Maryland, College Park, Maryland, USA
[61]Syracuse University, Syracuse, New York, USA
[62]Pontifícia Universidade Católica do Rio de Janeiro (PUC-Rio), Rio de Janeiro, Brazil
[associated with Universidade Federal do Rio de Janeiro (UFRJ), Rio de Janeiro, Brazil]
[63]University of Chinese Academy of Sciences, Beijing, China
(associated with Center for High Energy Physics, Tsinghua University, Beijing, China)
[64]School of Physics and Technology, Wuhan University, Wuhan, China
(associated with Center for High Energy Physics, Tsinghua University, Beijing, China)
[65]Institute of Particle Physics, Central China Normal University, Wuhan, Hubei, China
(associated with Center for High Energy Physics, Tsinghua University, Beijing, China)
[66]Departamento de Fisica, Universidad Nacional de Colombia, Bogota, Colombia
(associated with LPNHE, Université Pierre et Marie Curie, Université Paris Diderot, CNRS/IN2P3, Paris, France)
[67]Institut für Physik, Universität Rostock, Rostock, Germany
(associated with Physikalisches Institut, Ruprecht-Karls-Universität Heidelberg, Heidelberg, Germany)
[68]Van Swinderen Institute, University of Groningen, Groningen, Netherlands
(associated with Nikhef National Institute for Subatomic Physics, Amsterdam, Netherlands)
[69]National Research Centre Kurchatov Institute, Moscow, Russia
[associated with Institute of Theoretical and Experimental Physics (ITEP), Moscow, Russia]
[70]National University of Science and Technology "MISIS", Moscow, Russia
[associated with Institute of Theoretical and Experimental Physics (ITEP), Moscow, Russia]
[71]National Research Tomsk Polytechnic University, Tomsk, Russia
[associated with Institute of Theoretical and Experimental Physics (ITEP), Moscow, Russia]
[72]Instituto de Fisica Corpuscular, Centro Mixto Universidad de Valencia—CSIC, Valencia, Spain
(associated with ICCUB, Universitat de Barcelona, Barcelona, Spain)
[73]University of Michigan, Ann Arbor, Michigan, USA
(associated with Syracuse University, Syracuse, New York, USA)
[74]Los Alamos National Laboratory (LANL), Los Alamos, New Mexico, USA
(associated with Syracuse University, Syracuse, New York, USA)

[†]Deceased.
[a]Also at Università di Ferrara, Ferrara, Italy.
[b]Also at Laboratoire Leprince-Ringuet, Palaiseau, France.
[c]Also at Università di Milano Bicocca, Milano, Italy.
[d]Also at Università di Modena e Reggio Emilia, Modena, Italy.
[e]Also at Novosibirsk State University, Novosibirsk, Russia.
[f]Also at LIFAELS, La Salle, Universitat Ramon Llull, Barcelona, Spain.
[g]Also at Università di Bologna, Bologna, Italy.
[h]Also at Università di Genova, Genova, Italy.
[i]Also at Università di Pisa, Pisa, Italy.
[j]Also at Università di Bari, Bari, Italy.
[k]Also at Sezione INFN di Trieste, Trieste, Italy.
[l]Also at Università degli Studi di Milano, Milano, Italy.

[m]Also at Universidade Federal do Triângulo Mineiro (UFTM), Uberaba-MG, Brazil.
[n]Also at AGH—University of Science and Technology, Faculty of Computer Science, Electronics and Telecommunications, Kraków, Poland.
[o]Also at Università di Padova, Padova, Italy.
[p]Also at Università di Cagliari, Cagliari, Italy.
[q]Also at MSU—Iligan Institute of Technology (MSU-IIT), Iligan, Philippines.
[r]Also at Escuela Agrícola Panamericana, San Antonio de Oriente, Honduras.
[s]Also at Scuola Normale Superiore, Pisa, Italy.
[t]Also at Hanoi University of Science, Hanoi, Vietnam.
[u]Also at P.N. Lebedev Physical Institute, Russian Academy of Science (LPI RAS), Moscow, Russia.
[v]Also at National Research University Higher School of Economics, Moscow, Russia.
[w]Also at Università di Roma Tor Vergata, Roma, Italy.
[x]Also at Università di Roma La Sapienza, Roma, Italy.
[y]Also at Università della Basilicata, Potenza, Italy.
[z]Also at Università di Urbino, Urbino, Italy.
[aa]Also at Physics and Micro Electronic College, Hunan University, Changsha City, China.
[bb]Also at School of Physics and Information Technology, Shaanxi Normal University (SNNU), Xi'an, China.